An AC Electrokinetic Technique for Collection and Concentration of Particles and Cells on Patterned Electrodes

Ketan H. Bhatt,[†] Sonia Grego,[‡] and Orlin D. Velev[†,*]

Department of Chemical and Biomolecular Engineering, North Carolina State University, Raleigh, North Carolina 27695-7905 and RTI International, Research Triangle Park, North Carolina 27709

Received March 10, 2005. In Final Form: April 26, 2005

We report an electrohydrodynamic effect arising from the application of alternating electric fields to patterned electrode surfaces. The AC fields were applied to dilute suspensions of latex microspheres enclosed between a patterned silicon wafer and an ITO-coated glass slide in a small chamber. The latex particles became collected in the center of the conductive "corrals" on the silicon wafer acting as bottom electrode. The particle collection efficiency and speed depended only on the frequency and strength of the field and were independent of the material properties of the particles or the electrodes. The leading effect in the particle collection process is AC electrohydrodynamics. We discuss how the electrohydrodynamic flows emerge from the spatially nonuniform field and interpret the experimental results by means of electrostatic and hydrodynamic simulations. The technique allows three-dimensional microfluidic pumping and transport by the use of two-dimensional patterns. We demonstrate on-chip collection of latex particles, yeast cells, and microbes.

1. Introduction

The development of integrated microfluidic chips that can perform sample pretreatment and analysis on a single chip, also known as micro-Total Analysis Systems (μTAS), is still in its infancy and is an area of extensive research.[1−5] μTAS devices are adaptable for extensive parallelization and automation and have the potential to drastically reduce both the time and cost for analysis. Electric fields are well suited for use in such devices as they have the ability to transport, manipulate, and analyze most sample types including particles and cells. Forces of electrical origin that can be used in μTAS include electro-osmosis, dielectrophoresis (DEP) and AC electrohydrodynamics (EHD). These forces can be applied separately or simultaneously and their magnitudes can be easily adjusted by changing the amplitude or the frequency of the applied external field.

Dielectrophoresis is the interaction of an uncharged dielectric particle with a nonuniform electric field.[6−8] Particles are either attracted toward or repelled from the electric field maxima depending on their effective polarizability in the medium. DEP has been used by various researchers, including us, for forming linear aggregates of nanoparticles,[9−11] colloidal crystals,[12−15] and cell arrays.[16] In μTAS devices, DEP can be used as a tool for particle, cell, and DNA manipulation and separation.[17−21] Large amount of research has been devoted to Field Flow Fractionation on microfluidic chips, where DEP along with pressure driven flow is used to separate particles based on their dielectric properties.[22−24]

Electro-osmosis and AC electrohydrodynamics are electrokinetic effects arising from the interaction of ions in the electrical double layer formed on a surface and the tangential component of the electric field inside the double layer. Both these forces result in liquid flow and are suitable for pumping of liquids in μTAS devices.[25−29] AC electrohydrodynamics has been found to be a contributing force in colloidal crystal formation during electrophoretic

* Corresponding author. E-mail: odvelev@unity.ncsu.edu.
† North Carolina State University.
‡ RTI International, formerly MCNC Research & Development Institute.

(1) Reyes, D. R.; Iossifidis, D.; Auroux, P. A.; Manz, A. *Anal. Chem.* **2002**, *74*, 2623.
(2) Auroux, P. A.; Iossifidis, D.; Reyes, D. R.; Manz, A. *Anal. Chem.* **2002**, *74*, 2637.
(3) Erickson, D.; Dongqing, L. *Anal. Chem. Acta* **2004**, *507*, 11.
(4) Tudos, A. J.; Bessselink, G. A. J.; Schasfoort, R. B. M. *Lab Chip* **2001**, *1*, 83.
(5) Huang, Y.; Mather, E. L.; Bell, J. L.; Madou, M. *Anal. Bioanal. Chem.* **2002**, *372*, 49.
(6) Pohl, H. A. *Dielectrophoresis*; Cambridge University Press: Cambridge, 1978.
(7) Jones, T. B. *Electromechanics of Particles*; Cambridge University Press: Cambridge, 1995.
(8) Morgan, H.; Green, N. G. *AC Electrokinetics: Colloids and Nanoparticles*; Research Studies Press Ltd.: UK, 2002.
(9) Bhatt, K. H.; Velev, O. D. *Langmuir* **2004**, *20*, 467.
(10) Hermanson, K. D.; Lumsdon, S. O.; Williams, J. P.; Kaler, E. W.; Velev, O. D. *Science* **2001**, *294*, 1082.
(11) Khondaker, S. I.; Yao, Z. *Appl. Phys. Lett.* **2002**, *81*, 4613.
(12) Velev, O. D.; Kaler, E. W. *Langmuir* **1999**, *15*, 3693.
(13) Lumsdon, S. O.; Kaler, E. W.; Williams, J. P.; Velev, O. D. *Appl. Phys. Lett.* **2003**, *82*, 949.
(14) Lumsdon, S. O.; Kaler, E. W.; Velev, O. D. *Langmuir* **2004**, *20*, 2108.
(15) Gong, T.; Marr, D. W. M. *Langmuir* **2001**, *17*, 2301.
(16) Brission, V.; Tilton, R. D. *Biotechnol. Bioeng.* **2002**, *77*, 290.
(17) Zheng, L. F.; Brody, J. P.; Burke, P. J. *Biosens. Bioelectron.* **2004**, *20*, 606.
(18) Gascoyne, P. R. C.; Vykoukal, J. V. *P. IEEE* **2004**, *92*, 22.
(19) Gasycoyne, P.; Vykoukal, J. *Electrophoresis* **2002**, *23*, 1973.
(20) Gascoyne, P.; Mahidol, C.; Ruchirawat, M.; Satayavivad, J.; Watcharasit, P.; Becker, F. F. *Lab Chip* **2002**, *2*, 70.
(21) Markx, G. H.; Talary, M. S.; Pethig, R. *J. Biotechnol.* **1994**, *32*, 29.
(22) Giddings, J. C. *Science* **1993**, *260*, 1456.
(23) Wang, X. B.; Vykoukal, J.; Becker, F. F.; Gascoyne, P. R. C. *Biophys. J.* **1998**, *74*, 2689.
(24) Wang, X. B.; Yang, J.; Huang, Y.; Vykoukal, J.; Becker, F. F.; Gascoyne, P. R. C. *Anal. Chem.* **2000**, *72*, 832.
(25) Ajdari, A. *Phys. Rev. Lett.* **1995**, *75*, 755.
(26) Ajdari, A. *Phys. Rev. E* **2000**, *61*, R45.
(27) Brown, A. B. D.; Smith, C. G.; Rennie, A. R. *Phys. Rev. E* **2000**, *63*, 016305.
(28) Ramos, A.; Morgan, H.; Green, N. G.; Castellanos, A. *J. Colloid. Int. Sci.* **1999**, *217*, 420.
(29) Cabrera, C. R.; Yager, P. *Electrophoresis* **2001**, *22*, 355.

10.1021/la050658w CCC: $30.25
Published on Web 06/03/2005

deposition.[30−35] The term "induced-charge electro-osmosis" (ICEO) has recently been introduced to describe electrokinetic phenomena in which the applied electric field induces a charge on a conducting or a dielectric surface and the same field interacts with its own induced charge to produce fluid motion. Electro-osmosis and AC electrohydrodynamics can be classified as ICEO phenomena.[36]

Most microfluidic chips at present require that the samples containing the particles, cells, or molecules of interest are preconcentrated and precleaned. Sample pretreatment is labor intensive and generally requires benchtop equipment. Filtration or centrifugation can be a major source of artifacts, in particular, for cell analysis due to the interactions of the cells, particles, and contaminants in the concentrated cake.[37,38] Collection and preconcentration of cells thus remains a major problem in μTAS devices. Chips performing particle collection in a chamber using alternating electric field are being developed by various groups.[39−42] Bennet et al. used negative DEP and prevented particles in the chamber from crossing "dielectrophoretic gates", the region of high electric field intensity.[39] Suehiro et al. created a DEP filter by filling up the space between electrodes in the chamber with glass beads.[40] Yeast cells were attracted to the areas of high electric field intensity on the surface of the glass beads. In both these chips the collected particles were flushed out from the chamber by switching off the applied field. A drawback of these DEP-based chips is that they rely on the dielectric properties of the particles and cells and thus are not applicable to all sample types. Electrokinetic flows on the other hand are not dependent on the dielectric properties of the particles, and thus they can be applied to all sample types. Hoettges et al. and Wong et al. have developed chips that combine EHD flow with DEP for particle collection on planar electrodes in small chambers.[41,42]

This paper describes a new electrokinetic technique that uses AC electric fields for collecting particles using patterned electrodes in a small chamber. The effect of various process parameters on the collection speed and efficiency are investigated. These parameters include the applied field strength and frequency, the electrolyte and particle concentration, the particle size and charge, and the pattern geometry. We extend an EHD flow model to describe the particle collection process. The experimental results are interpreted by means of numerical simulations of the electric field and fluid velocity distribution in the chamber. The technique and the results of the model could be used to design chips that collect and concentrate particles, yeast cells, and microbes from dilute suspensions.

(30) Yeh, S.; Seul, M.; Shraiman, B. I. *Nature* **1997**, *386*, 57.
(31) Trau, M.; Saville, D. A.; Aksay, I. A. *Langmuir* **1997**, *13*, 6375.
(32) Solomentsev, Y.; Bohmer, M.; Anderson, J. L. *Langmuir* **1997**, *13*, 6058.
(33) Guelcher, A.; Solomentsev, Y.; Anderson, J. L. *Powder Technol.* **2000**, *110*, 90.
(34) Nadal, F.; Argoul, F.; Hanusse, P.; Puligny, B.; Ajdari, A. *Phys. Rev. E* **2002**, *65*, 061409.
(35) Sides, P. J. *Langmuir* **2003**, *19*, 2745.
(36) Bazant, M. Z.; Squires, T. M. *Phys. Rev. Lett.* **2004**, *92*, 066101.
(37) Fung, D. Y. C. *Comprehens. Rev. Food Sci. Food Safety* **2002**, *1*, 1.
(38) Noble, R. T.; Weisberg, S. B. *J. Water Health*, in press.
(39) Bennett, D. J.; Khusid, B.; James, C. D.; Galambos, P. C.; Okandan, M.; Jacqmin, D.; Acrivos, A. *Appl. Phys. Lett.* **2003**, *83*, 4866.
(40) Suehiro, J.; Zhou, G.; Imamura, M.; Hara, M. *IEEE T. Ind. Appl.* **2003**, *39*, 1514.
(41) Hoettges, K. F.; McDonnell, M. B.; Hughes, M. P. *J. Phys. D Appl. Phys.* **2003**, *36*, L101.
(42) Wong, P. K.; Chen, C. Y.; Wang, T. H.; Ho, C. M. *Anal. Chem.* **2004**, *76*, 6908.

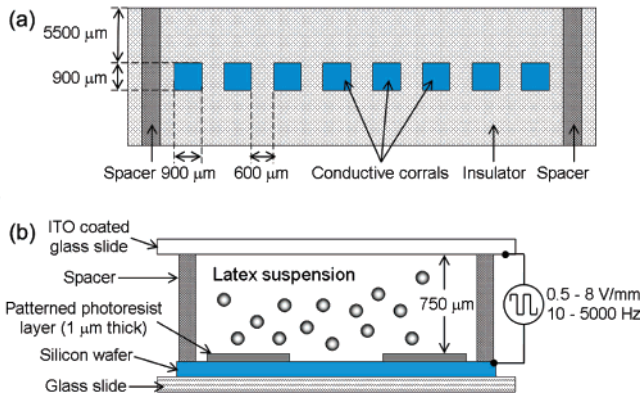

Figure 1. Schematics of (a) the patterned silicon wafer and (b) the experimental setup of the chamber used for particle collection.

2. Materials and Methods

Experimental Apparatus. Electric field was applied to latex particles suspended in a chamber by means of a patterned silicon electrode and an indium−tin oxide (ITO) electrode separated vertically by a spacer. The schematics of the patterned silicon wafer and the experimental setup are shown in Figure 1. A 1 μm thick layer of Shipley positive photoresist was deposited on a p-doped silicon wafer. The silicon wafer had sufficient conductivity (nominally $\rho = 1-20\ \Omega$ cm) to act as an electrode, and the photoresist layer served as an insulator. The photoresist layer was patterned using standard photolithography techniques to expose parts of the underlying silicon wafer as shown in Figure 1a. The pattern consisted of eight squares approximately 0.81 mm^2 in area, separated by 600 μm of photoresist-covered surface. These patterned squares acted as conductive corrals surrounded by the insulating photoresist layer. This patterned silicon wafer served as the bottom electrode in the experimental chamber (Figure 1b). A glass slide coated with transparent conductive ITO layer was used as the top electrode for the chamber. The two electrodes were separated by a 0.75 mm silicone rubber spacer (Grace Bio-Labs, OR) with openings for adding and removing particle or cell suspensions from the chamber. The volume of the chamber formed was approximately 120 μL.

The silicon wafer and the top ITO electrode were connected to electrical leads using Circuit Works CW2400 conductive epoxy (Chemtronics, GA). The leads were connected to an Agilent 33120A 15 MHz function generator (Agilent Technologies, CO) providing AC signal 2−10 V in peak to peak magnitude. The strength of the applied field and the current passing through the chamber were measured using multimeters connected in the circuit. The maximum currents measured in our experiments (~0.2 mA) were one order of magnitude lower than the maximal permissible current load of the Agilent function generator, and the voltage was very stable. We connected an oscilloscope to the circuit and observed no capacitive distortion of the square wave signal when the load (experimental chamber) was connected into the circuit. The particles in the chamber were continuously monitored using Olympus BX-61 microscope equipped with reflection-mode and fluorescent-mode microscopy, and images were recorded using Olympus DP-70 digital CCD camera.

Materials. Fluorescent latex microspheres of different diameters were purchased from Molecular Probes (Eugene, OR). The particles were centrifuged and washed twice with deionized water from Millipore RiOs system to remove any preservatives, surfactants, or electrolytes present in the media. The washed samples were diluted using deionized water to obtain latex suspensions with final particle concentration of 0.01% w/v particles. The conductivities of latex suspensions thus prepared were within the 0.05−0.07 μS/cm range. Sodium chloride was purchased from Fisher Scientific (Pittsburgh, PA), and phosphate-buffered saline (PBS) tablets were purchased from Sigma-Aldrich (St. Louis, MO). A PBS solution containing 1.37 mM NaCl, 0.027 mM KCl, and 0.1 mM phosphate buffer was prepared by dissolving one PBS tablet in 20 L of deionized water. Bakers' yeast (dried, active) was purchased from MP Biomedicals, Inc. (Aurora, OH). The yeast cells were dispersed in the PBS

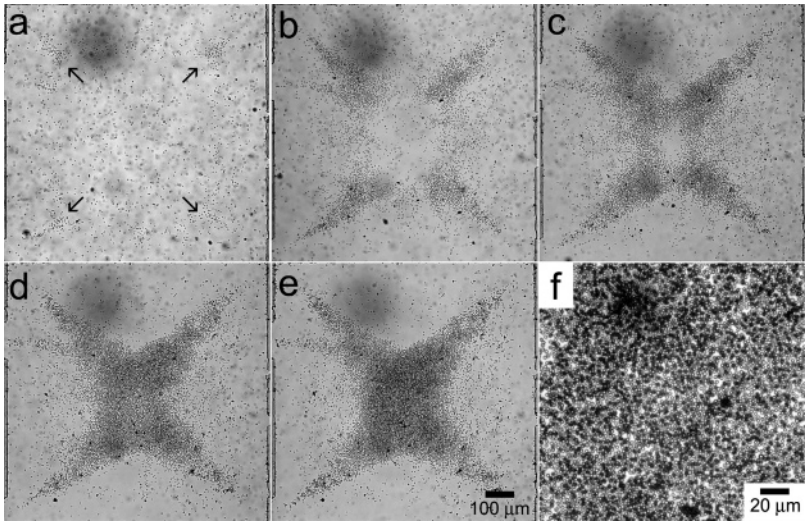

Figure 2. Time-lapse images of 2 μm latex particles collected from a 0.01% w/v suspension without added electrolyte in one conductive corral at a frequency of 100 Hz and a field strength of 2.67 V/mm. (a) $t = 1$ min, the arrows show areas where particles began accumulating, (b) $t = 15$ min, (c) $t = 30$ min, (d) $t = 45$ min, (e) the equilibrium point, $t = 60$ min. (f) Zoom in micrograph at the center of the corral shows that the particles are loosely packed.

solution to obtain a final concentration of 0.014% w/v yeast. The conductivity of latex suspensions with 0.5 mM NaCl added was 6.15 μS/cm and that of yeast suspensions in PBS was 17.5 μS/cm.

3. Results

When an alternating electric field was applied to the chamber, the suspended latex particles began accumulating inside the conductive corrals on the bottom electrode. The particles near the photoresist-corral edges began moving into the corrals, whereas the particles farther away from the corral edges on the photoresist surface remained stationary. Observing the particles with the 50× objective and following their three-dimensional motion, we found evidence for fluid flow. Close to the photoresist surface, the particles clearly moved toward the conductive corrals; whereas, when the microscope stage was adjusted such that the plane of focus was elevated above the photoresist surface, most particles exhibited Brownian motion but a few were observed to be moving away from the corrals. The velocity of particles moving into (or toward) the corrals exceeded the velocity of particles moving away from the corrals. Many more particles were moving toward the corrals than moving away, so that over time the originally suspended latex particles collected at the centers of all conductive corrals inside the chamber.

Typical results for collection of 2 μm latex particles in one of the conductive corrals when an alternating field was applied are shown in Figure 2. A digital movie of the process is available as Supporting Information. Inward fluid flow was generated around the corral edge immediately upon the application of the electric field. Within seconds the particles driven by fluid flow started moving into the conductive corral. The first results of particle accumulation were visible near the corral corners one minute after the start of the experiment (these regions are marked by arrows in Figure 2a). As time went by, more latex particles from the sides were pushed inward into the corral. The particles accumulated near the corral edges were pushed further toward the center (Figure 2b–d). One hour after the start of the experiment the particle accumulation was mostly completed, and no further collection of particles was observed (Figure 2e). Upon closer inspection it was found that the amount of particles moving into the corral close to the photoresist surface was balanced by the amount of particles moving away from the corral in horizontal planes some distance away from the photoresist surface. The collected particles formed an "X-shaped" accumulation pattern with four spikes corresponding to the four corners of the conductive corral. A small fifth spike (to the top left) in the observed particle accumulation pattern corresponds to a small notch in the corral edge illustrating the importance of the boundary area. At the center of the conductive corral, the particles were loosely packed (Figure 2f) and did not form a closed packed crystal structure as in the previously reported case of electrophoretic deposition on patterned electrodes.[43,44]

Effect of Operating Parameters. To understand the particle accumulation process we characterized in detail the effect of different operating parameters on the process. The collection process was found to be affected by the frequency and strength of the applied field and concentration of electrolyte in the suspension. The effects of these three controlling parameters are described in detail below. We also investigated a number of other operating parameters, including particle size (varied from 200 nm to 5 μm), particle charge (negative sulfate latex and positive amidine latex), concentration of particles in the suspension (0.001−0.1% w/v), corral size (1−115 mm^2), and substrate material (silicon and gold). *We did not observe any difference in the process of particle accumulation or in the collection pattern in the corral when these operating parameters were varied in the ranges listed above.*

Effect of Applied Field Strength. We varied the strength of the applied field in our experiments from 0.5 to 8 V/mm. The particle velocity increased on increasing the external voltage, which resulted in increased particle accumulation. Physical breakdown of the photoresist layer and deterioration of the conductive corrals took place when the applied voltage was increased beyond 8 V/mm. The collection pattern inside the corral remained unchanged on increasing the strength of the applied field.

The particle velocity near the photoresist-corral edge was measured for different applied voltages using video microscopy. Series of micrographs were taken using a 50× objective and the digital camera attached to the microscope. Time-lapse images were acquired for a total time

(43) Hayward, R. C.; Saville, D. A.; Aksay, I. A. *Nature* **2000**, *404*, 56.
(44) Gong, T.; Wu, D. T.; Marr, D. W. M. *Langmuir* **2003**, *19*, 5967.

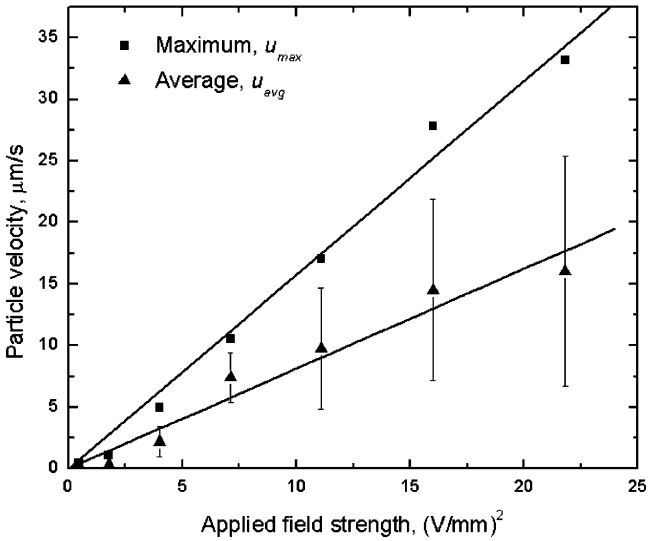

Figure 3. Particle velocities measured by video microscopy near photoresist-corral edges at 100 Hz. The lines are linear fits for (top) maximal particle velocity and (bottom) average particle velocity.

of one minute, with one second interval between the frames. Digital movies of the moving particles are available as Supporting Information. The image subtraction function in Adobe Photoshop was used to calculate the particle coordinates and velocity. Two frames in gray scale modes were superimposed, and the second frame was subtracted from the first one resulting in one single image. Particles which did not move during the time between the two frames (typically stuck to the surface) were thus eliminated from the resulting image. The moving particles were visible as white or black circles that stood for their beginning and ending positions, respectively. The distances traveled by each particle were then calculated from their coordinates in the image, and the velocities were obtained by dividing them by the time difference between the two frames.

For each applied voltage between 0.67 and 4.67 V/mm, we measured the velocity of a minimum of one hundred particles using this procedure. The maximum particle velocity and the average particle velocity were found to be proportional to the square of the applied field strength. The plots of the maximal particle velocity and the average particle velocity as a function of the squared applied voltage are shown in Figure 3. The least-squares fit for the coefficient of linear dependence was 1.57×10^6 $\mu m^3/(V^2 s)$ and 0.81×10^6 $\mu m^3/(V^2 s)$ respectively for the maximum and average particle velocities. Particle velocity as high as 50 μm/s can be obtained with 5.33 V/mm applied field. For applied voltages higher than 5 V/mm, the particles move so fast that there are not enough particles remaining within the field of view of the digital camera in consecutive frames and hence the above outlined procedure for measuring particle velocity could not be used. The data will be discussed in the model section below.

Effect of the Field Frequency. Particle collection took place when the frequency of the applied field was between 10 and 5000 Hz. At low frequencies (<10 Hz) and at high frequencies (>5000 Hz), no fluid flow was observed and no collection of particles occurred. For the range of frequency where particle collection was observed (10−5000 Hz), the rate of particle accumulation diminished with increasing frequency. Experimental images for the collection of particles on a single conductive corral for two different frequencies, 2000 and 5000 Hz, are compared in Figure 4. The voltage of the applied field was 4 V/mm at 2000 Hz and 6.67 V/mm at 5000 Hz. Also compare these images with Figure 2e, where particles are collected at 2.67 V/mm, 100 Hz. Although the higher field should have increased the rate of collection of particles as described above, the amount of particles collected at 5000 and 2000 Hz were significantly lower than that at 100 Hz. At higher frequencies the particles also stayed close to the periphery of the conductive corrals rather than collecting at their centers.

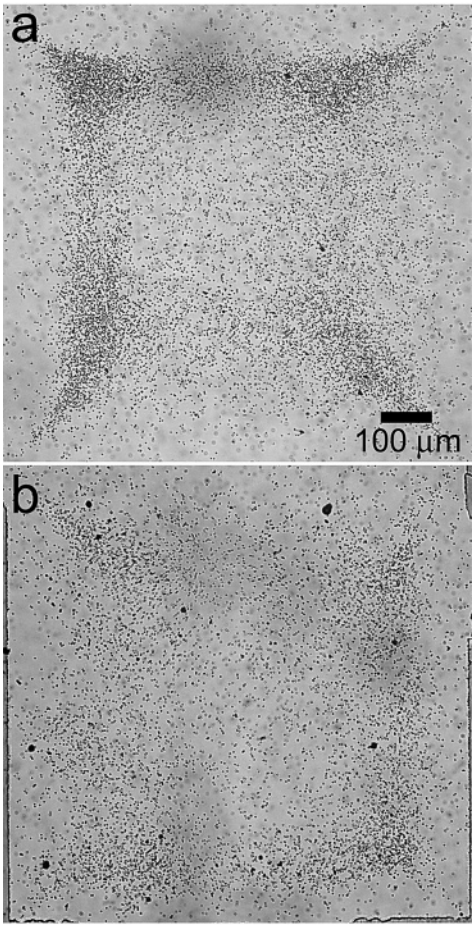

Figure 4. Effect of the frequency of the applied field (a) 2000 Hz, 4 V/mm, (b) 5000 Hz, 6.67 V/mm. Both images show collection of 2 μm latex from 0.01% w/v suspensions and were taken 1 h after the start of the experiment. Compare also with Figure 2e.

Effect of Electrolyte Concentration. We studied the effect of different concentrations of sodium chloride on the collection of latex particles inside the corrals. At electrolyte concentrations larger than 2 mM NaCl there was no particle collection and no observable fluid flow. For suspensions with less than 2 mM NaCl, the rate of particle collection remained approximately the same as suspensions without added electrolyte. However, the accumulation pattern formed was significantly different in the presence of electrolyte. The particles collected in the centers packed more closely when electrolyte was added. Typical experimental images for the process in suspensions containing 0.5 mM NaCl are shown in Figure 5. The micrographs were taken from the particles collected in the center of a conductive corral 1 h after the start of the experiment. The close ("quasi-crystal") packing is obvious when these images are compared with Figure 2e and 2f (showing structure of the particles collected without added electrolyte).

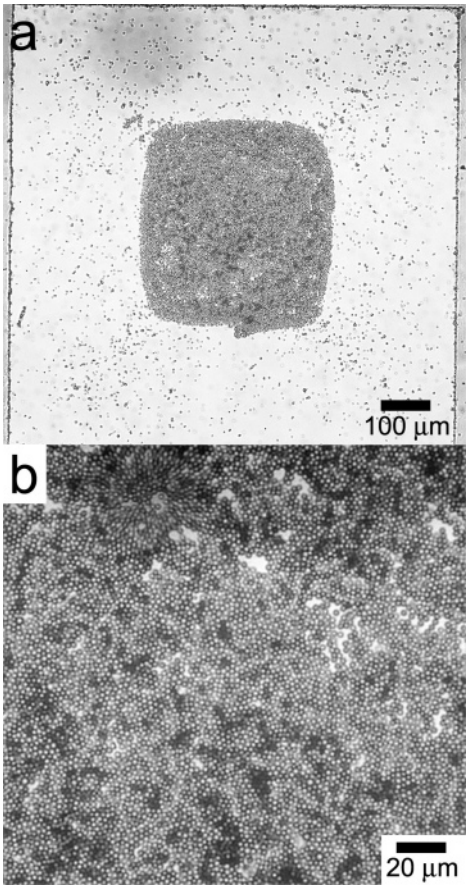

Figure 5. Particle collection for 2 μm, 0.01% w/v latex suspensions with 0.5 mM NaCl under electric field of 4 V/mm, frequency of 100 Hz. (a) $t = 1$ h, particles pack more closely compared to suspensions without electrolyte (compare with Figure 2e). (b) Zoom in image at the center of the corral shows close packed colloidal quasi-crystals (compare with Figure 2f).

The addition of the electrolyte also increased the adhesion of the particles to the surface of the silicon wafer. For experiments without electrolyte, the collected particles were easily removed when the chamber was flushed with water. However, when electrolyte was added to the suspensions almost half of the particles collected in the corral remained on the surface when the chamber was flushed with water. These particles remain adherent to the silicon wafer even after drying the chamber.

4. Interpretation of Results and Discussion

The forces that are exerted on the particles when an alternating electric field is applied to the chamber could include dielectrophoresis (acting directly on them) and AC electrohydrodynamics (moving them together with the surrounding liquid). The transport and collection of particles in the conductive corrals can be attributed to either or both of these forces, so it is necessary to analyze the results in order to distinguish which effects are predominant.

Dielectrophoresis. Dielectrophoresis is the interaction of a particle with a nonuniform field, and its magnitude is given by[6−8]

$$|F_{\mathrm{DEP}}| = 2\pi\epsilon \mathrm{Re}|K(\omega)|R^3\nabla(E^2) \qquad (1)$$

where R is the radius of the particle, ϵ is the dielectric constant of the medium, E is the electric field intensity, and K is the Clausius−Mossoti factor, the effective

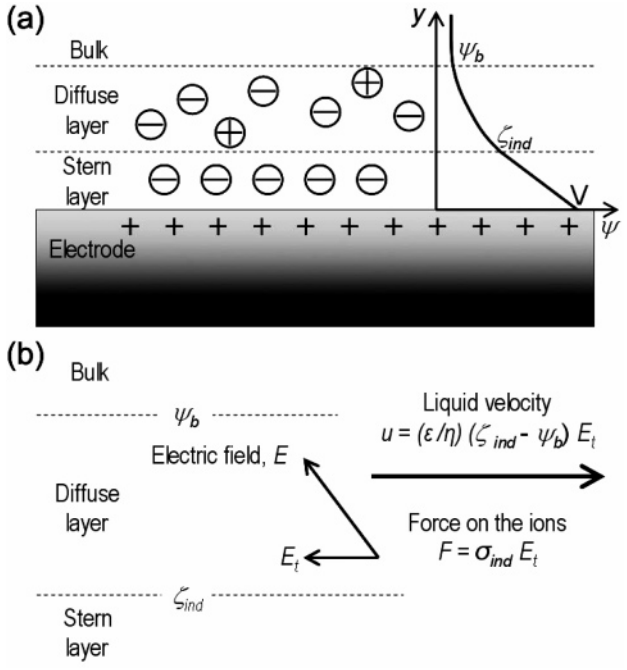

Figure 6. (a) Schematics of the electrical double layer formation on an electrode surface for the positive half-cycle of the applied AC field. (b) The induced charge in the double layer σ_{ind} interacts with the tangential electric field E_{t} to generate electrohydrodynamic flow.

polarizability of the particle. K is dependent on the frequency of the applied field, ω. For $\mathrm{Re}(K) > 1$ the particles are attracted toward the electric field maxima, and for $\mathrm{Re}(K) < 1$ the particles are repelled from the electric field maxima. For latex particles in water at frequencies less than several MHz, the DEP force is always positive and the particles are attracted toward the areas of high electric field intensity.[7]

AC Electrohydrodynamics. Particles may also be transported by the motion of the surrounding liquid upon application on an alternating electric field. AC electrohydrodynamics is an effect arising from the interaction of the ions in the double layer formed on a surface with an applied electric field and results in liquid motion and particle transport.[8,45,46] When a charged surface is in contact with an electrolyte solution, counterions of charge opposite to the surface charge are preferentially attracted toward the surface forming the electrical double layer[45] (Figure 6). The layer of ions closest to the surface is called the Stern layer and is usually 1−2 nm thick. The ions in the Stern layer are specifically adsorbed and are considered effectively bound to the surface.[46] Counterions in the outerlying diffuse layer are not bound to the surface and can diffuse in and out of the layer to the bulk solution or can move transversely along the surface. The plane between the Stern layer and the diffuse layer is known as the outer Helmholtz plane, and its potential is termed ψ_d. It has been proven that the outer Helmholtz plane and the slip plane associated with the tangential motion of liquid on a charged surface (in electrokinetics) are in most cases closely situated.[46] Consequently, for practical purposes ψ_d can be approximated with the electrokinetic potential at the slip plane, ζ.[46] Typical magnitudes of ζ are of the order of 100 mV. The effective charge density

(45) Hunter, R. J. *Foundations of Colloid Science*; Oxford University Press: Oxford, 2001.
(46) Lyklema, J. *Fundamentals of Interface and Colloid Science Volume 2: Solid−Liquid Interfaces*; Academic Press Inc.: San Diego, 1995.

of the diffuse double layer is conveniently approximated by[45]

$$\sigma = -\epsilon\kappa(\zeta - \psi_b) \tag{2}$$

where ψ_b is the potential in the bulk solution and $1/\kappa$ is the Debye length of the suspension. $1/\kappa$ depends on the temperature and the bulk electrolyte concentration. The thickness of the diffuse double layer is usually of the order of $3/\kappa$ to $4/\kappa$. If a tangential electric field is applied to the surface, the ions in the diffuse layer experience a Columbic force that leads to their movement. The ions in turn drag the liquid surrounding them resulting into a net fluid motion. This electrokinetic effect is well-known as electroosmosis and the fluid velocity is given by

$$u = -(\epsilon/\eta)(\zeta - \psi_b)\boldsymbol{E}_t \tag{3}$$

where η is the viscosity of the medium and E_t is the tangential electric field. If there are particles present in the solution, they will be dragged by the fluid flow and the particle velocity will be approximately equal to the fluid flow velocity.

If instead of a DC field a tangential AC field is applied to the surface there will be no net movement of the liquid, because the fluid velocity in one-half-cycle will exactly cancel out the opposite velocity in the other half-cycle of the AC field. However, if the surface is itself connected to an electrical circuit and behaves as an electrode, there will be an added charge on the surface, which will increase its intrinsic charge during one-half-cycle and reduce it during the another half-cycle of the electric field. Depending on the intrinsic charge of the surface and the external voltage applied, the *induced* zeta potential under the action of the applied electric field, ζ_{ind}, will be higher or lower compared to the intrinsic zeta potential ζ and will be different for the positive and negative half-cycles. If the external voltage applied is V,

$$\zeta^+_{ind} = \zeta + aV \text{ for the positive half-cycle}$$

$$\zeta^-_{ind} = \zeta - aV \text{ for the negative half-cycle} \tag{4}$$

where $0 < a < 1$.

As the fluid velocity is proportional to the zeta potential, the magnitude of fluid velocity in consecutive half-cycles of the applied field will be different and not cancel each other. The result is a net fluid motion on the electrode surface. This fluid motion is termed as AC electrohydrodynamics (EHD). We will show below that this effect occurs near the edge of the photoresist in our system.

Simulation of Electric Field and Fluid Velocity Distributions. To understand how dielectrophoresis and AC electrohydrodynamics might be involved in the particle collection process, it is necessary to determine the direction and magnitude of these forces in the chamber. Both forces are related to the magnitude and direction of the electric field, and hence we need to model the electric field distribution inside the experimental system. As the corral geometry is symmetric and all corrals within the chamber are identical, it is sufficient to simulate the field distribution on only one conductive corral and the surrounding photoresist. We simulated the electric field inside the chamber during the positive half-cycle of the applied voltage with 2D electrostatic calculations using the FEMLAB multiphysics modeling package (COMSOL, Burlington, MA).

The calculation of the electric field in FEMLAB required several steps. The geometry of the system to scale was specified as a side view of the chamber as shown in Figure 7. The dielectric subdomains were water ($\epsilon = 80$) and the photoresist layer ($\epsilon = 2$). The boundaries were the bottom silicon electrode (applied voltage = 1.5 V, positive half-cycle of the AC field) and the top ITO electrode (grounded). The two boundaries to the left and right were taken to be electrically symmetrical. Next the solution space was triangulated into a conformal mesh. The physical properties inside the elements remain constant, and hence there are no mesh elements across subdomains or boundaries. The solver was then initialized to solve the Poisson equation for all elements to obtain the electric field distribution. The electrical field vectors inside the chamber computed with FEMLAB are shown in Figure 7b.

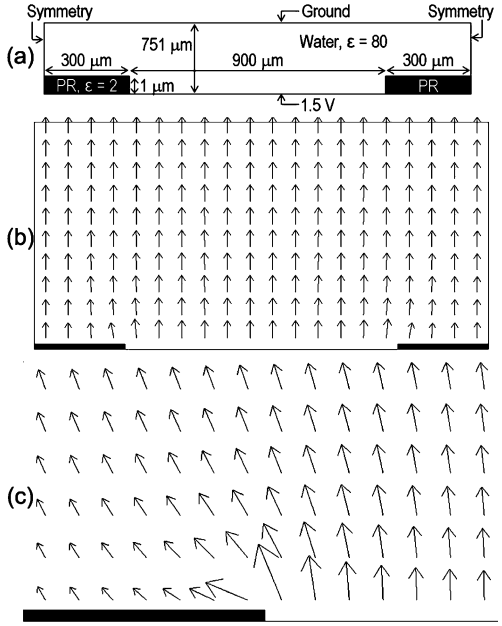

Figure 7. Simulation of the electric field distribution inside the chamber using FEMLAB. (a) Boundary conditions and geometry specified, (b) electric field vectors calculated for one conductive corral, (c) zoom-in near the left photoresist-corral edge shows nonuniform field distribution. Black boxes illustrate the photoresist layer and are not to scale except in part c.

The electric field inside the chamber is mostly uniformly vertical as seen in Figure 7b. However, there are small areas of nonuniformity near the photoresist-corral edges. Zoom-in of the area of nonuniformity in the electric field distribution close to the left photoresist-corral edge is shown in Figure 7c. The magnitude of the electric field, as determined by the length of the vectors, is highest near the photoresist-corral edge and decreases as we move away from edge. The first implication from these calculations is that there will be a local field gradient, which could attract the particles dielectrophoretically toward the corral edge. However, if DEP were the controlling force, the particles would collect at the photoresist-corral edge and not inside the corral as seen in the experiments. The nonuniform field also does not exert any force on the bulk fluid medium but acts only on the suspended particles. This could not explain the fluid circulation observed inside the chamber under the application of the electric field. Thus, we rule out the possibility of dielectrophoresis as the major controlling force, due to the lack of evidence for particle attraction to the areas of highest field gradient.

We now consider the alternate hypothesis that AC electrohydrodynamics is responsible for particle collection inside the chamber. To ascertain this, we need to identify the surfaces where *field-induced* electrical double layer is formed (in addition to intrinsic surface charging), and then we need to calculate the tangential electric field on

these surfaces. Double layer formation takes place both on the silicon wafer surface and on the photoresist surface. At the silicon wafer surface (of the conductive corral), for, e.g., the positive half cycle of the alternating electric field, negative counterions from solution are added to the electrical double layer. The photoresist layer behaves as a capacitor with the bottom electrode and the photoresist-solution interface acting as opposing plates. Thus, a positive half-cycle voltage applied at the bottom electrode also creates a negative charge build up in electrical double layer at the top photoresist-solution interface.

During the positive half-cycle of the electric field, the induced additional charge in the double layer will be negative. At the photoresist surface the tangential field is directed toward the corral and is stronger at its edges (see Figure 7c). Thus the *induced* negative ionic charges in the double layer will be dragged toward the corral, generating an EHD flow in the same direction (the direction of the electric field and the sign of charge in the diffuse layer are similar to those depicted in Figure 6, and hence the direction of flow). During the negative half cycle of the AC wave, the field on the electrode will be negative, the induced double layer charge will be positive, and its interaction with the tangential field will *again lead to EHD flow toward the corral*. Thus, there will be constant EHD "pumping" along the gradient of the field, which will occur only at the corral edges. No EHD flow will be generated in the middle of the corral, in the middle of the photoresist, or on the top ITO electrodes as the fields there are uniform.

The magnitude of the EHD flow can be estimated from the magnitude of the tangential electric field. We computed the values of the tangential electric field at the patterned electrode surface from the FEMLAB simulation of the electric field distribution. The plot of the tangential component of the electric field on the bottom electrode surface versus the distance from the photoresist-corral edge is shown in Figure 8a. The tangential component of the field is highest at the photoresist edge and decreases rapidly as we go away from the edge toward the photoresist surface. The tangential field inside the conductive corral is zero. The velocity of the generated EHD flow should increase from zero some distance away from the corral edge to reach its maximum at the edge and then decrease in the corral due to friction and lack of driving force. The particle velocity will be the same as the EHD flow. The particles may also face dielectrophoretic attraction toward the edge, which further decreases the particle velocity.

The above model-predicted relation between particle velocity and the distance from the photoresist-corral edge was verified experimentally by video microscopy measurements. The procedure followed was similar to that described in the Results section. In addition to calculating particle velocities, we measured the distances from the photoresist-corral edge along the direction of particle motion. The experimentally measured particle velocity as a function of the distance from the photoresist-corral edge for applied field of 2 V/mm, 100 Hz, is plotted in Figure 8b. The particles entrained by the EHD flow were accelerated as they arrive closer to the edge of the corral, and their velocity reached a maximum at the corral edge in exact correspondence with the EHD model and simulations. After they crossed the corral edge, the particle velocity decreased, as there is no tangential field gradient and no EHD driving force. Movies of the particle velocity at three different distances from the photoresist-corral edge illustrating the particle velocity profile are available in AVI format as Supporting Information.

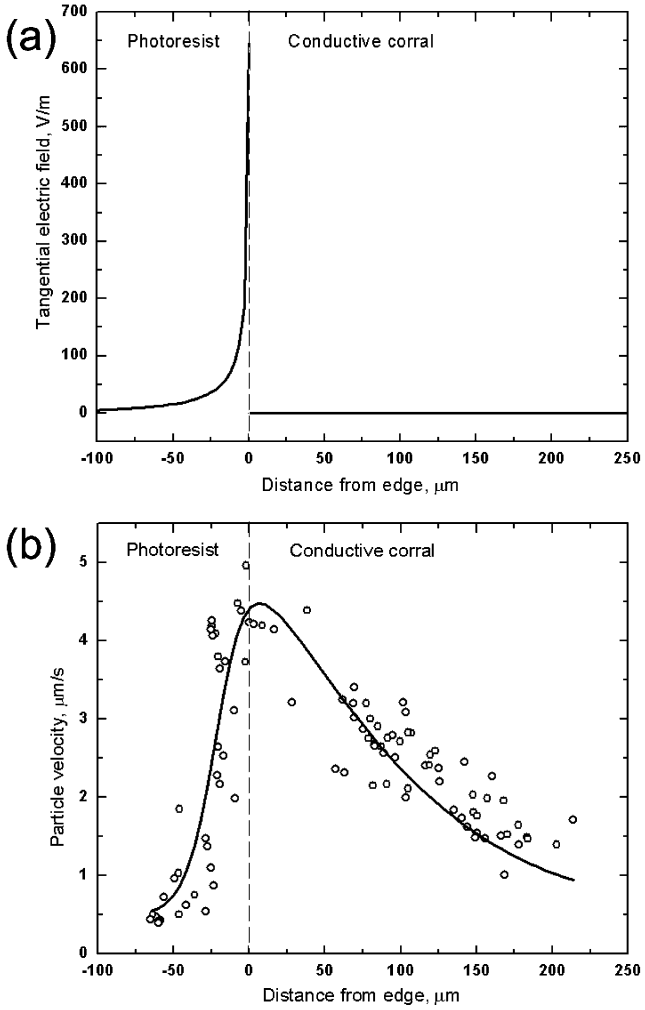

Figure 8. (a) Computed tangential electric field from FEMLAB simulation and (b) experimentally measured particle velocities. The comparison proves that the particles (and liquid) get accelerated in area of high tangential field outside the conductive corral edge.

AC electrohydrodynamics explains well the fluid motion and particle dynamics in the proximity of the conductive corral. To model how this EHD "pump" generates macroscopic fluid flow in the cell, we used FEMLAB to simulate the fluid velocity distribution in the chamber. The geometry used for this simulation was similar to the one for the electric field distribution (Figure 9a). In this case there was only one subdomain, water, with hydrodynamic properties as follows: density = 1000 kg/m^3 and viscosity = 10^{-3} kg m^{-1} s^{-1}. To simulate the EHD flow generated on the photoresist surface, we set the surface velocity spanning 100 μm inside the photoresist edge equal to 4 μm/s (approximate highest particle velocity at the edge obtained experimentally in Figure 8b, shown by red arrows in Figure 9a). The fluid velocity distribution inside the chamber was then obtained by solving the Navier−Strokes equations. The resulting velocity distribution is shown in Figure 9b. The EHD flow generated on the photoresist surface results in bulk circulation of the fluid inside the chamber, which corresponds to the experimental observations. The simulation also shows that there is a stagnant region at the center of the conductive corral, where the particles were experimentally observed to collect.

The results obtained from the FEMLAB simulations of the electric field distribution and the fluid flow point out that the major driving factor of the effects observed is the EHD flow. It drags and accelerates the particles as they

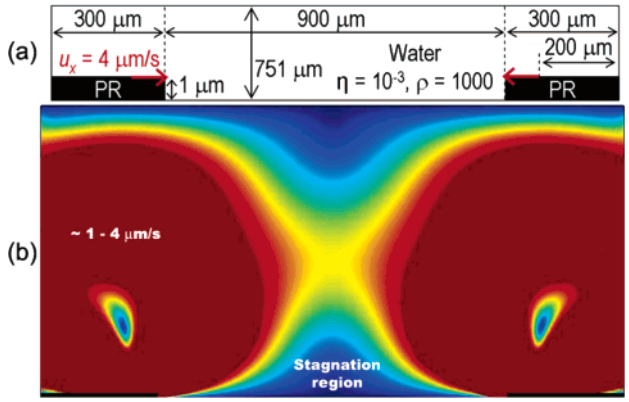

Figure 9. Simulation of the fluid velocity distribution inside the chamber using FEMLAB (a) Boundary conditions and the geometry specified, (b) computed velocity distribution inside the chamber. The liquid is accelerated at the corral edges and drags along the particles which are deposited in the stagnation region in the middle.

approach the corral edge and pushes them toward the center of the corral. The particles settle in the center of the conductive corral where there is a stagnant flow region. DEP is not a leading force, but it may contribute by attracting the particles toward the photoresist-conductive corral edge, where they are entrained in the flow.

We are now ready to interpret the experimentally observed effect of different operating parameters on the particle collection process in terms of the above-described model. The expected electrohydrodynamic behavior and the experimental observation for different operating parameters are compared in Table 1.

The EHD flow is dependent on the induced charge in the double layer and on the tangential electric field. Any operating parameter which affects either of these parameters will affect the EHD flow and consequently the particle collection inside the chamber. If the applied external field, E, is increased, the induced zeta potential will increase, $(\zeta - \psi_b) \propto E$ (compare with eq 4 and ref 8) The tangential component will also increase linearly with the total electric field, $E_t \propto E$.[8] The fluid velocity and hence the particle velocity which are proportional to the induced zeta potential multiplied by the tangential electric field (eq 3) thus should increase as the applied voltage squared, $u \propto E^2$, as was experimentally observed (Figure 3). This is an established relation for many polarization-dependent electric fields driven effects.[28]

The effect of the applied field frequency on the particle collection process can be explained by the dynamics of the double layer formation process. For an alternating electric field the induced component of the double layer is formed by negative counterions in the positive half-cycle and by positive counterions in the negative half-cycle. The ions in the solution have to diffuse in and out of the double layer to the bulk solution with the change of sign of the alternating electric field. When the applied electric field frequency is high (of the order of few kHz), the ions do not have enough time to redistribute as the field goes from one-half-cycle to the next.[8,45] The induced charge in the double layer at high frequencies hence is zero, and so there should be no EHD flow and no particle collection. On the other hand, when the applied field frequency is very low (of the order of a few Hz), the ions have enough time to form the double layer and suppress the field. The entire potential drop at low-frequency (or static) fields takes place in the double layer.[8,45] The electric field inside the chamber will be zero and again there should be no EHD flow. The effect of frequency is similar to the one previously observed for aggregation of particles due to EHD flow.[47]

In the experiments we observed that there is no particle collection for applied field frequency <10 Hz or >5 kHz, which is in accordance with the above concepts. Within the 10 Hz to 5 kHz range we found that the rate of particle accumulation decreased as the frequency of the applied field was increased (see Figure 4). As described above, the ions in the double layer need a finite time to redistribute with the changing sign of the field. As the applied field frequency is increased, the time available for redistribution decreases which results into a decrease in the amount of the induced charge in the double layer.[8,45] The EHD flow at the surface hence will decrease as the frequency is increased, and the particle collection will diminish.

For suspensions with high electrolyte concentration, the large amount of ions present in the bulk solution will lead to a dense double layer that suppresses the applied field similarly to the case of low frequency. The entire potential will then drop within the thin double layer, the tangential electric field will not be able to drag excess ions outside the shear plane, and no EHD flow will be generated. Correspondingly, we observed that there is no collection of particles for suspensions with NaCl concentrations greater than 2 mM. For suspensions with NaCl concentrations less than 2 mM, we observed that the particles pack closely compared to the suspensions without the electrolyte. The closer packing of the particles (and stronger adhesion to the substrate) can be attributed to the decreased electrostatic repulsive forces between the particles.

The model based on EHD flow is conceptually similar to the earlier research on flows around and interactions between particles on electrodes.[30−36] The new element in this work is the use of patterned surfaces leading to macroscopic circulation flows within the experimental chamber, rather than local flows around particles. Our model depends on only two parameters, the induced charge in the double layer and the presence of tangential field inside the double layer. The EHD-based collection does not depend on particle charge or size, the corral geometry, or the electrode material, and indeed we observed experimentally that these parameters do not affect the particle collection. The good correlation between the expected electrohydrodynamic behavior and the experimental result (Table 1) confirms the model.

5. Potential Applications of the EHD Flow Technique

This new electrokinetic technique could have many potential applications in μTAS devices. One important application area is particle and cell collection and concentration from dilute suspensions. The EHD flow can also be used for pumping of fluids in microfluidic devices. The excellent correlation obtained between the EHD flow model and the experimental observation of particle collection can be utilized in predicting particle behavior on electrodes patterned with photoresist layers of various sizes and shapes. We demonstrate two such applications of this new electrokinetic technique below.

EHD Focusing of Particles. The detection and analysis of particles or cells in μTAS devices generally require that the analytes of interest be concentrated or "focused" in a small area that is coincident with the foci of fluorescence illuminators and detectors. Such "particle focusing" using EHD flow was demonstrated by modifying

(47) Ristenpart, W. D.; Aksay, I. A.; Saville, D. E. *Phys. Rev. E* **2004**, *69*, 021405.

Table 1. Expected Electrohydrodynamic Behavior and Experimental Observations for Particle Collection under Different Operating Parameters

parameter	range studied	expected EHD behavior	experimental observation
AC voltage	0.5−8 V/mm ↑	$u \propto E^2$	$u \propto E^2$
AC frequency	<10 Hz	$E_t = 0$, $u = 0$	$u = 0$
	10 Hz to 5 kHz ↑	ζ_{ind} ↓	u ↓
	>5 kHz	$\zeta_{ind} = 0$, $u = 0$	$u = 0$
electrolyte concentration	0.5−2 mM NaCl ↑	Debye length ↓	Particles more closely packed
	>2 mM NaCl	$E_t = 0$, $u = 0$	$u = 0$
particle charge	positive or negative	↔	↔
particle size	200 nm to 5 μm	↔, but larger particles may experience more friction	higher voltage required for collection of larger particles
corral area	1−115 mm^2	↔	↔
substrate material	silicon or gold	↔	↔

the conductive patterns in the chamber. We replaced the eight square conductive corrals on the bottom electrode by one large 12 mm diameter circular corral. The chamber spacer dimensions were still maintained at 20 × 13 × 0.75 mm^3 ($L \times W \times H$), cropping the pattern to the shape shown in Figure 10. The particle collection process was similar to that for the smaller square conductive corrals; however, the pattern formed by collected particles was quite different. Initially the particles pushed into the corral from all sides and collected close to the periphery of the corral forming a concentric ring of concentrated particles. As time went by, the ring was pushed inward and the asymmetric distribution of particles along the two axis of the chamber resulted in a pattern of two concentrated regions, Figure 10. Effectively, the result is that the two concentrated particle regions are formed at the foci of the curved arcs seen in the image. By bringing the two arcs closer to each other and decreasing the corral size, one can focus particles in one single concentrated region. On the other hand, if the arcs are so designed that there is an unbalanced fluid flow from different sides of the corral, chips that translate particles in one direction and result in a net pumping of liquid may be fabricated. EHD focusing and pumping has large advantages in μTAS devices as it has the possibility of generating fluid circulation within the chamber by applying electric fields of low strength.

Collection of Live Cells. Microfluidic chips for cell collection and manipulation are of large interest for bioanalytical applications.[3,4,18] For example, in water monitoring systems there is a need for chips that can concentrate microorganisms or cells of interest present in very dilute concentrations.[38] The EHD flow generated in our experiments is not dependent on the physical properties of the particles, and hence the technique can be easily adapted to preconcentration and focusing of live cells from suspension. We demonstrated this by collecting yeast cells from a diluted phosphate buffer saline (PBS) solution using EHD flow. Optical image of yeast cell collection from dilute suspensions in one conductive corral under the application of 8 V/mm, 100 Hz electric field is shown in Figure 11. The larger size of the yeast cells (5 μm compared to 2 μm for the particles) required a higher applied voltage. The surrounding solution contains approximately 1.37 mM NaCl, 0.027 mM KCl, and 0.1 mM phosphate buffer, and the presence of electrolyte led to the formation of quasi-packed array of yeast cells similar to the quasi-colloidal crystals obtained with latex particles. The advantages of collecting cells in a close packed area, where they can be easily examined and eventually discriminated by type, are obvious.

We also successfully performed preliminary experiments on *Enterococcus faecalis*, common microbes from river water samples. The microbes of initial concentration 10 000 cells/mL were successfully collected at the center of the square conductive corrals (images and data not shown here). Thus, we have proven that our electrokinetic technique is suitable for collection of cells and microbes from dilute suspensions and can be used in microfluidic chips for bioanalytical purposes, among other possible applications.

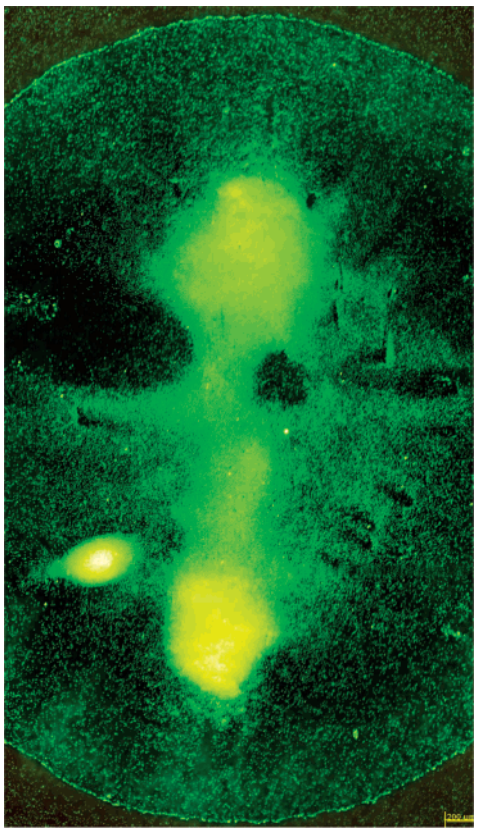

Figure 10. EHD focusing: 2 μm latex particles collected using 4 V/mm, 100 Hz alternating electric field for 75 min at the foci of the 12 mm diameter circular corral.

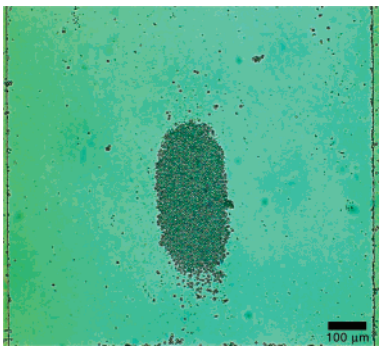

Figure 11. Micrograph of yeast cells collected in a conductive corral from a suspension containing 0.0141% solids under an alternating electric field.

6. Conclusions

The new electrokinetic technique reported here allows collection and concentration of colloidal particles suspended in a chamber using a combination of AC electrohydrodynamics and dielectrophoresis. This technique was found to be applicable to particles, cells, and bacteria irrespective of their size, shape, or charge, as it is only dependent on the formation of the double layer at the electrode surface and not on the physical properties of the suspended particles. The EHD model and the FEMLAB electrostatic and hydrodynamic simulations were consistent with the experimental observations. The effect is strong, easy to control, and may be of importance in many microfluidic and μTAS systems. The EHD simulations can be used to understand and predict flows generated in corrals of various sizes and shapes and may be exploited in designs of patterned electrodes for microfluidic pumping. This technique has potential in various μTAS devices as it can easily be combined with various detection and analysis methods, especially if they are based on electric fields. We demonstrated microfluidic chips that are capable of focusing latex particles and collecting yeast cells from buffer solutions.

Acknowledgment. Prof. Rachel Noble of UNC—Chapel Hill kindly provided the river water samples containing *Enterococcus faecalis*. This study was supported by NER and CAREER grants from the National Science Foundation and by the Camille and Henry Dreyfus Foundation. S.G. gratefully acknowledges the support from DARPA through SPAWARSYSCEN Grant Number N66001-03-1-8900.

Supporting Information Available: Movies (in AVI format) illustrating particle collection in the conductive corral over time and particle velocity at different distances from the photoresist-corral edge. This material is available free of charge via the Internet at http://pubs.acs.org.

LA050658W